RECORDSOF CHEMICAL SCIENCES

Synthesis and Characterization of Magnetite (Fe3O4) Nanoparticles from Iron Sand as a Catalyst in Biodiesel production using waste cooking oil.

[1*]Samaila Muazu Batagarawa, [1]Ahmed Lawal Mashi, [1]Sada Bello

https://doi.org/10.33003/frscs_2024_0303/01

Accepted: 27th July, 2024
Published: 12th August, 2024

1. Department of Pure and Industrial Chemistry, Umaru Musa Yar'adua University, Katsina, Katsina State

**Corresponding Author:*
Prof. Samaila Muazu Batagarawa
samaila.muazu@umyu.edu.ng

FRsCS Vol.3 No. 3 (2024)
Official Journal of Dept. of Chemistry, Federal University of Dutsin-Ma, Katsina State.
http://rudmafudma.com

ISSN (Online): 2705-2362
ISSN (Print): 2705-2354

Abstract

Iron sand is a readily available natural material. This study involved the extraction of magnetite (Fe_3O_4), an iron oxide material, from locally accessible iron sand. co-precipitation method was employed using hydrochloric acid and ammonium hydroxide. The characterization methods for the catalysts were XRD, SEM, FTIR, and Magnetic susceptibility. From the XRD analysis, 76% of the sample appeared as hematite but changed to magnetite (55%) when activated and 25% as hematite. Furthermore, the extracted Fe3O4 was used as a catalyst for producing biodiesel from waste cooking oil. The variables studied were the catalyst loading (0.25-2.00 g) and duration of reaction (200 m). The results revealed that all parameters influence the transesterification experiment for biodiesel production. FT-IR, basic back titration, and ASTM methods characterized the biodiesel produced. Optimization of reaction parameters was performed, and a maximum yield of 97.3% was obtained using the conditions of a 1.125 g catalyst load, a 6:1 methanol to oil ratio, 115 minutes of reaction time, and a reaction temperature of 65 °C. After one cycle of catalyst regeneration, a 92% yield was obtained. Remarkably, a yield of 97.3% was obtained when the transesterification reaction was carried out according to the model's recommended conditions, which was in line with the model's predicted value

Keywords: Magnetite, Haemetite, Biodiesel, Heterogeneous catalyst, recycle

Introduction

Catalysts play a significant role in the transesterification of vegetable oils. In large-scale applications, these catalysts are expected to be cost-effective and environmentally friendly. Iron sand is one of the most widely used magnetic materials in many fields including; electronics, energy, chemistry, a catalyst, and medical diagnosis. Heterogenous catalysts have the advantage of being recycled in addition to their green nature. Iron sand which is rich in Fe content is generally oxidized and forms iron oxide, such as Fe_3O_4 magnetite, hematite (α-Fe_2O_3), and maghemite (γ-Fe_2O_3) (Andimutiafitri, 2018). So far, the utilization of natural iron sand has not been optimal in the study area, that is, it is only limited to being used as building material. Recently, magnetic nanoparticles such as magnetite have gained enthusiastic attention from many researchers due to their unique properties on a nanoscale, such as a large surface area, high surface energy, low toxicity, good biocompatibility, superparamagnetic behavior, high absorption, and transfer electrons (Rahmawati, 2018). The conventional process for biodiesel production is transesterification or alcoholysis (typically methanolysis), by which the triglycerides are reacted with alcohols (typically methanol), in the presence of a catalyst, either homogeneous or heterogeneous, as a reaction promoter, to produce fatty acid methyl esters (FAME) (Mahlia, 2020).

Biodiesel is produced using the transesterification or alcoholysis process, which is usually facilitated by acids, bases, enzymes, and other types and forms of catalysts (Ong, 2014). The catalysts can be either in a homogeneous or in a heterogeneous phase as of the reactants. The choice of appropriate catalyst depends on several factors which include the amount of free fatty acids (FFAs) in the oil and the water content among others. The main aim of this research work is to synthesize magnetite (Fe_3O_4) from locally available sand and investigate its catalytic activity as a heterogeneous catalyst in biodiesel production.

Table 1: Various precursors for magnetite synthesis

Precursor	Magnetite/Hematite Produced	Preparation method	Reference
Iron sand	85% Fe_3O_4	Mechanical	(Nabgan, et al., 2022)
Iron sand	77% Fe_3O_4	Co-precipitation	(Ong, et al., 2014)
Iron sand	34% Fe_2O_3	Ball milling	(Prameswari, et. al., 2022)
Iron sand	69.8% Fe_2O_3	Co-precipitation	(Widodo, et al., 2020)
Iron sand	70% Fe_2O_3	Co-precipitation	(Adak, et al., 2020)
Iron sand	Fe_3O_4	Co-precipitation	(Najmi, et al., 2024)
Iron sand	Fe_3O_4	Co-precipitation	(Safitri, et al., 2021)
Iron sand	Fe_3O_4	Co-precipitation	This research work

Materials and Methods

Iron Sand collection and pretreatment

Natural iron sand was collected from a beach of River Fanga in Batagarawa town, Batagarawa local government area of Katsina state, Nigeria (Fig.1), The iron sand was collected using a permanent magnet. The sample was carefully transferred to a pre-cleaned plastic container, labeled with a date and place of sampling, properly tightened, and brought to the laboratory for further treatment. While in the laboratory, other residual/adhering (metallic and non-metallic) materials were handpicked out of the bulk iron sand and discarded.

Sample preparation

The iron sand sample was ground to powder using mortar and pestle and then sieved with a 100nm mesh sieve size to obtain the finest magnetic powder. The sieved powder was thoroughly washed with distilled water and oven-dried at 120 ºC for 18 hours. The resultant powder was refluxed at 75 ºC using 10% HCl for 2hrs followed by washing with distilled water until neutral pH and then oven-dried at 95 ºC for 18hrs

The equation below shows the reaction sequence:

$3Fe_3O_4(s)+8HCl(l)\rightarrow FeCl_2(l)+2FeCl_3(l)+3Fe_2O_3(s)+3H_2O(l)+H_2(g)$

Co-precipitation method

To the above mixture, 50 ml NH_4OH solution was added and allowed to stand for 1 hour to obtain a precipitate. The solution formed a solid black precipitate which was washed with distilled water several times so that the results obtained were completely clean from impurities. The precipitate was oven-dried at 120°C for 2 hrs to remove water molecules and later activated at 70° C for 3 -The co .hrsprecipitation and activation processes is shown below

$2FeCl_3(l)+FeCl_2(l)+H_2O(l)+8NH_4OH(l)\rightarrow Fe_3O_4(s)+8NH_4F(l)+5H_2O(l)$ (Najmi et al., 2024 & Safitri et al., 2021).

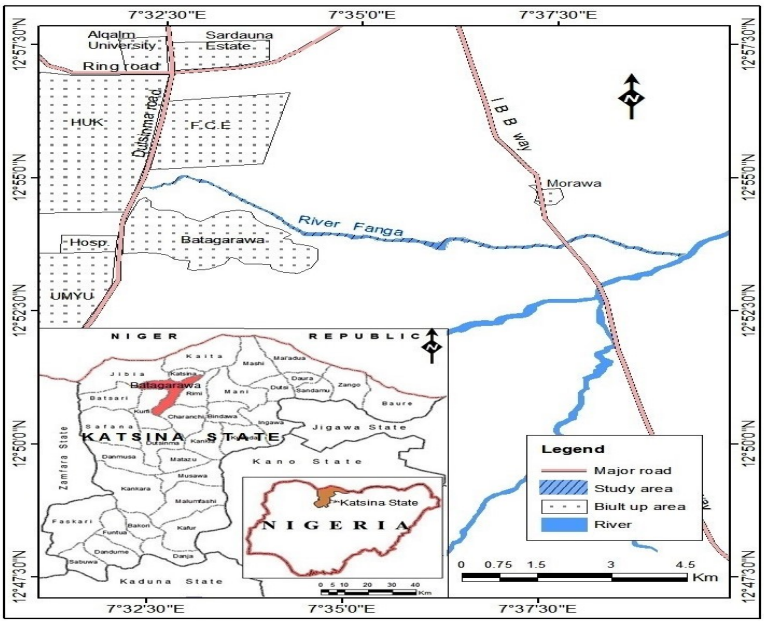

Fig. 1: Map showing Sampling Area.

(Source: National Aeronautic and Space Administration Spot Image, (2020)

Catalyst Characterizations

The prepared catalysts (Freshly prepared, Activated, and Recycled) were subjected to various characterization methods for analysis as follows:

X-ray diffraction (XRD) analysis was carried out using an XRD-6000 diffractometer with Cu Kα radiation (λ=1.56 amstron, 30 kV, 30 mA). The phase identification was carried out by comparison with available d-spacing information and peaks from the graph.

Scan Electron Microscope Analysis (SEM): The analysis was used to study the microscopic structure and surface morphology of the particles. A Spectrophotometer, (phenom Prox 80007334) at an accelerating voltage of 15kV, beam size of 3.0, working distance of 10, and magnification of 1000, was used to determine the size and morphology of the particles.

Fourier Transform Infrared Spectroscopy (FT-IR) Analysis: The analysis was used to reveal all the functional groups present in the prepared samples. The samples were placed directly into the infrared beam of the FT-IR Spectrophotometer (VERTEX 70/70V, Agilent Technologies).

Magnetic Susceptibility: Magnetic susceptibility balance (Sherwood Scientific Limited, UK Serial No. 29275) was used to verify the magnetic properties of the extracted Fe_2O_3 powder. The Procedure reported by (Fahlepy et al., 2019) was adopted as follows:

$$Magnetic\ susceptibility\ (X_g) = \frac{C_{Bal}(L)(R-R_o)}{10^9 M}$$

Where; C_{Bal} = Balance calibration constant =1.0, L= Height of the sample in tube (cm), R =Reading obtained for tube + sample, R_0 = Reading for empty tube, M = Mass of the sample (g), also M= W_2-W_1, W_1 = weight of empty capillary tube by analytical balance, W_2 = Weight of capillary tube + sample.

From the knowledge of gram magnetic susceptibility (X_g), molar magnetic susceptibility (X_m) can be calculated using the relation; $X_m = (X_g) \times$ (Molar mass)

or, effective magnetic moment (μ_{eff}) = $\sqrt{Xm\ x\ T}$

Where; μ_{eff} = Effective magnetic moment, X_m = Molar magnetic susceptibility and
T = Absolute temperature,

The magnetic moment of the extracted sample was, therefore, calculated as X_m = (X_g) × (molar mass).

Collection and Pretreatment of Used Oil

The Used Cooking Oil (UCO) which has been used for frying snacks and other fast foods such as fried Yam and Chicken was collected from Barmo Ventures, a restaurant located at the Students Centre of the Umaru Musa Yar'adua University campus. Larger particles such as pieces of fried yam, egg, and vegetables were removed by passing through a sieve. The oil sample was allowed to settle for two (2) days after which it was filtered using a 100nm sieve to remove any suspended food particles and other inorganic residues. It was then heated at 110°C for 2h to remove water content (Nabgan, et al., 2022).

Experimental procedure

The used cooking oil was obtained from Barmo Restaurant in Umaru Musa Yaradua University Campus, as the raw material. Before the biodiesel production, the UCO was pre-treated to remove the water and impurities by heating it to 100 °C for 40 min and filtrating. The %FFA content of the filtrate was then determined using acid-base titration (Prameswari et al., 2023). First, 5 ml of methanol (99.98%, Merck, Germany) was added to 5 ml of WCO and added with 2 drops of Phenolphthalein indicator. The mixture was titrated with 0.1 N NaOH until a pink color persisted. The following equation was used to calculate the FFA content:

$$\%FFA = \frac{NaOH\ Vol.(ml) * NaOH\ Normality(N) * Fatty\ Acid\ Molecular\ weight}{density\ of\ UCO * Volume * 1000}$$

A series of batch experiments were conducted following the procedure reported by Angassa *et al*., (2023). The catalyst (Fe_2O_3) dosage used were as follows; 0.25, 0.50, 0.75, 1.00, 1.25, 1.50, 1.75 and 2.00g. The reaction temperatures used were as follows; 40, 50, 60, 70, 80 and 90 °C. The methanol/oil molar ratio was set as 1:3, 1:4, 1:5, 1:6, 1:7, 1:8 and 1:9. The reaction time was varied as 30, 45, 60, 90, 110, 140, 170 and 200 min. The % yield of the biodiesel produced from these preliminary experiments was calculated using Equation 1. The effect of these parameters on the biodiesel yield and conversion was calculated using Equation 2

$$\text{percentage conversion} = \frac{\text{amount of biodiesel produced}}{\text{amount of used oil taken}} x100 \quad \text{---equ 2}$$

Physico-Chemical Properties of Biodiesel Produced

To investigate the standard fuel properties of the biodiesel produced the procedure reported by Angassa et. al. (2023) was adopted as follows:

Specific Gravity

A 10 ml specific gravity bottle was used to carry out the specific gravity. The pre-weighted bottle was filled with the fuel sample to its brim and the final weight of the bottle was taken to give the weight of the sample which when divided by 10 gave the specific gravity and the density of the sample.

Pour Point

For the pour point, the sample was kept in an ultra-low temperature Refrigerator of -80°C with a test tube. The fluidity was checked after every 5 °C drop in temperature by bringing out the sample and checking. The particular temperature, at which the liquid ceases to flow, is known as the pour point, and this was recorded.

Flash Point

Pensky Martin Apparatus was used to determine the flash point. 30 ml of the sample was collected in the apparatus cup and cooled using a water bath. Stirring was done continuously during the process. After every 1°C fall in temperature, the vapor of the sample was exposed to a flame. The flashpoint is the point at which fire starts with a flash.

Kinematic Viscosity:

The sample was placed in a calibrated capillary glass viscometer tube, and held at a closely controlled temperature. The time required for the specific volume of the sample to flow through the capillary under gravity was measured; this time is proportional to the kinematic viscosity of the sample.

Response Surface Methodology

Response Surface Methodology (RSM) with a four-level factorial Box-Bahnken Design (BBD) of Design Expert software version 6.0.11 was employed. The design factors are; Catalyst loading (A), Reaction Time (B), Reaction Temperature (C) and Methanol to Oil volume ratio (D). The software gave twenty-nine experiments as shown in Table 2 :

Results and Discussion

X-Ray Diffraction (XRD) Analysis

The various phases present in the fresh, activated and regenerated catalysts were investigated using X-ray Diffractogram. The results for the fresh, activated and reused samples are presented in Table 3. Among them, the hematite phase appeared highest in fresh and present in small amounts in activated and reused samples. The activated form of the catalyst existed largely in magnetite, hematite and quartz phases, which shows that it is important for the sample to be activated before use to obtain the magnetite phase as shown by the XRD peaks in Fig. 2.

The composition of the various phases is presented in Table 3. The fresh catalyst consisted of Hematite (76%), Orthoclase (13%) and Magnetite (8.5%), while the activated sample consisted of Hematite (25%) Quartz (20%), Magnetite (55.1%), and Spessartine (10.6%), the re-used catalyst has the following composition; Spessartine (23%), Hematite (22%), Orthoclase (20%) and Magnetite (21%). The metal oxide content in a region varies depending on several factors such as geographic region, weather, and geologic conditions (Uzun et al., 2012). Iron sand deposits on the south coast of Yogyakarta comprise magnetite and maghemite minerals with levels of 59.97%, 11.7%, 6.48%, 4.34%, and 4.66% for Fe_2O_3, SiO_2, TiO_2, Al_2O_3, and CaO, respectively (Nugraha et al., 2016).

Fourier Transformed-Infra Red (FT-IR) Analysis

The functional groups present in the extracted samples of the iron sand were investigated using FT-IR. The results of the Analysis for the fresh, activated and recycled catalysts are given in Figures 3, 4 &5 respectively.

A peak at 3839 cm^{-1} and 3675 cm^{-1} indicated an absorption band typically corresponding to the stretching vibration of O-H from adsorbed water. The spectral region of 1796 cm^{-1} and 1632 cm^{-1} indicated the presence of a carbonyl group (C=O) stretching vibrations commonly in ketones, aldehydes, or carboxylic acids. A strong absorption at 1026 cm^{-1} indicated the presence of Si-O stretching vibration.

From the spectra of the activated catalyst (figure 4), the absorption band at the 3123 cm^{-1} region suggested the presence of O-H stretching vibration due to the adsorption of water. Similarly, the large broadband at 3369 cm^{-1} in the re-used sample (fig. 5) is ascribed to the O-H stretching vibration often found in water, alcohols or phenol.

The absorption bands around 2922cm^{-1} and 2847cm^{-1} are due to the C-H stretching. The sharp peak at 1736 cm^{-1} is associated with the stretching vibration of a carbonyl group (C=O) and the peaks at a region of 1595 cm^{-1} correspond to a C=C stretching vibration typically found in alkenes. However, the strong band below 700 cm^{-1} is related to FeO stretching mode.

Table 2: Four-level factorial Box-Bahnken design

	Factor 1	**Factor 2**	**Factor 3**	**Factor 4**
Run	**A: Catalyst Load (g)**	**B: Reaction time (m)**	**C: Reaction Temperature (^{o}C)**	**D: M/O Ratio**
1	1.125	115	65	6
2	2	115	65	3
3	1.125	30	90	6
4	2	30	65	6
5	1.125	115	65	6
6	2	115	90	6
7	0.25	30	65	6
8	1.125	200	65	3
9	0.25	115	65	3
10	1.125	200	90	6
11	1.125	200	40	6
12	1.125	115	90	3
13	1.125	115	65	6
14	1.125	115	90	9
15	0.25	115	40	6
16	1.125	30	65	3
17	1.125	30	65	9
18	1.125	200	65	9
19	0.25	200	65	6
20	1.125	115	65	6
21	1.125	115	40	9
22	1.125	30	40	6
23	2	115	40	6
24	1.125	115	65	6
25	2	115	65	9
26	2	200	65	6
27	0.25	115	90	6
28	1.125	115	40	3
29	0.25	115	65	9

Table 3: The various phases of the extracted samples from XRD Analysis

Phase/catalyst	Fresh	Activated	Re-used
Hematite	76	25	22
Orthoclase	13	-	20
Quartz	0.02	20	-
Anthophyllite	0.076	-	-
Geothite	-	12.8	15
Spessartine	-	10.6	23
Magnetite	8.5	55.1	21
Ilmenite	-	8.4	-

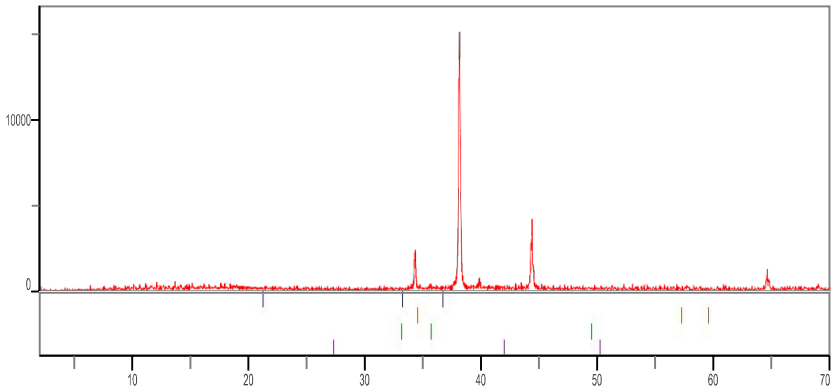

Figure 2: XRD spectra of the activated catalyst.

Scanning Electron Microscopy Analysis

The Scanning Electron Microscope (SEM) analysis of the fresh, activated, and regenerated catalysts was conducted to identify the morphological conditions and homogeneity of the samples, result for the three catalysts; fresh (a) activated(b) and re-used(c) are presented in Fig 6.

Table 4: Magnetic Susceptibility Analysis of the Freshly (a) and Regenerated (b) catalysts

S/N	Catalyst	X_g (a.m^2)	X_m (gmol^{-1})	μ_{eff}	Magnetic property
1	Fresh	$3x10^{-12}$	$4.791x10^{-10}$	$6.55x10^{-3}$	Para magnetic
2	Recycled	$3x10^{-12}$	$4.791x10^{-10}$	$6.55x10^{-3}$	Para magnetic

Table 5: Fuel Properties of the Biodiesel Produced

Property	Value
Density(at 40^{o}C)	0.886
K. Viscosity	4.8
Free fatty Acid	0.11
Acid Value	0.256
Specific gravity	0.878

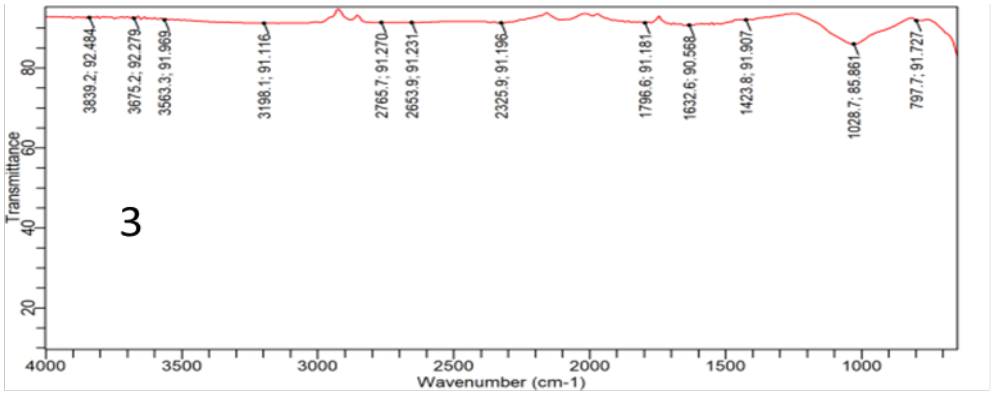

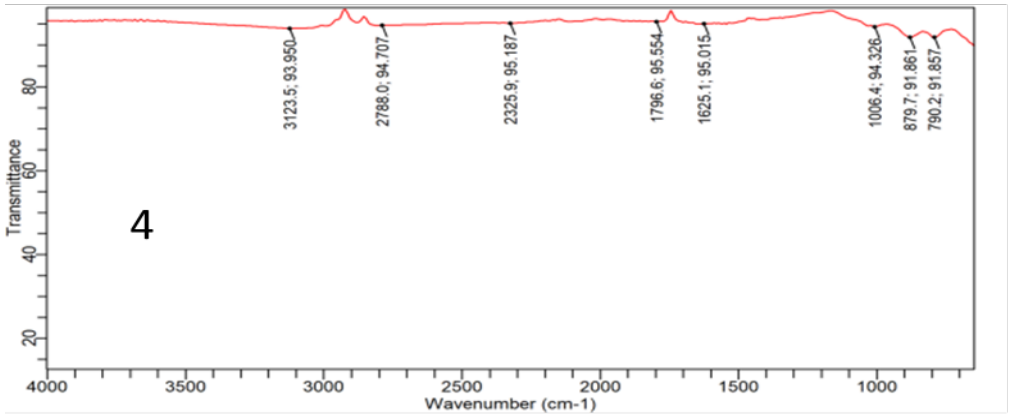

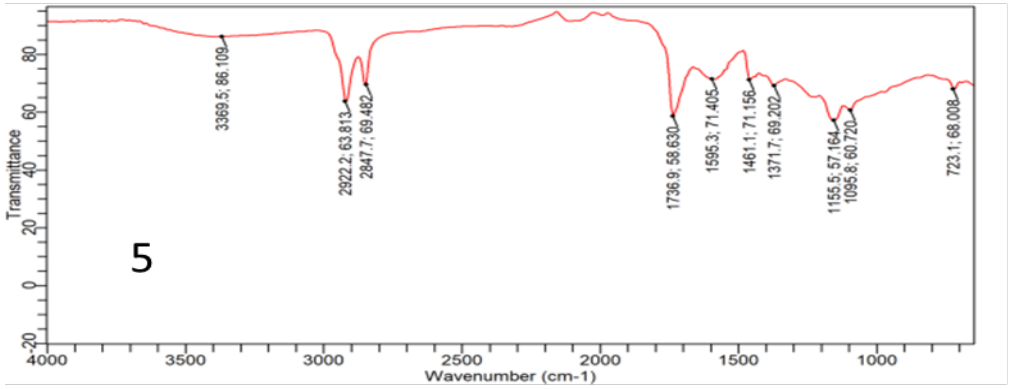

Fig. 3, 4, 5: FT-IR Spectrum of freshly prepared catalyst

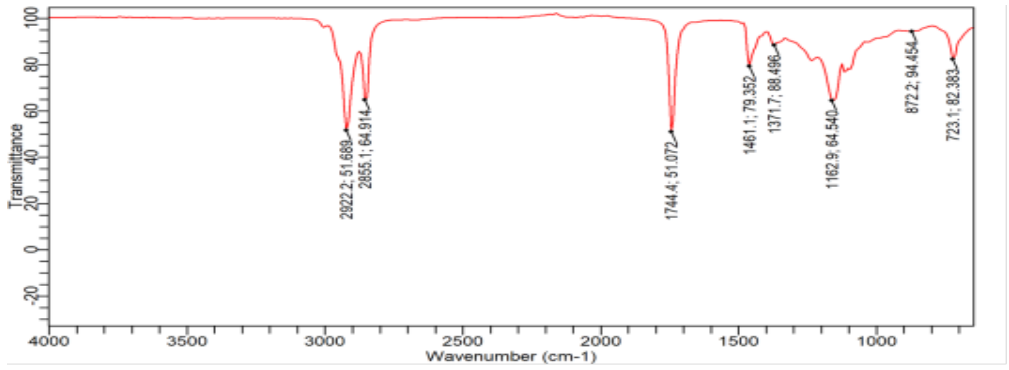

Fig. 7: FT-IR Spectrum of the produced biodiesel

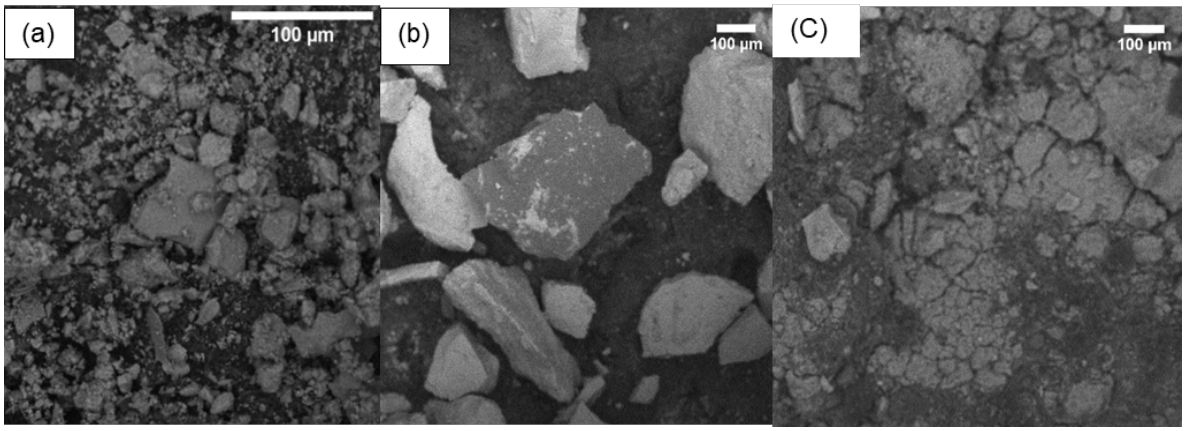

Fig 6: SEM images of the fresh catalyst (a), activated catalyst (b), and recycled catalyst (c).

The images showed agglomerated particles of the silica and possible interaction with the iron oxide. It can be seen clearly that, the activated form displayed some larger and whitish particles, probably consisting of the particles of FeO. The reused catalyst did not indicate any positive change from the fresh material, thus reflecting similar characteristics with the fresh catalyst.

Magnetic Susceptibility Measurement

The magnetic properties of the fresh and recycled catalysts were measured using magnetic susceptibility balance (Sherwood Scientific Limited UK, 29275). The result is presented in Table 4. The result of the magnetic susceptibility measurement of the fresh and the recycled (c) catalysts is presented in Table 6. The values were used to deduce the magnetic properties of the samples extracted from the iron sand. The results revealed that both the activated and re-used samples are paramagnetic. These values of mass susceptibility are within the range of mass susceptibility for magnetite (Yulianto et al., 2023).

Biodiesel Characterization and Analysis

The prepared catalyst was applied in the transesterification of used vegetable oil, and the biodiesel obtained was characterized by FTIR analysis and tested for physicochemical properties. The FT-IR spectra obtained are presented in Figure 7 and the properties are presented in Table 7. Similarly, images of the biodiesel produced are also presented in Figure 8. The FTIR indicated strong absorption at 2999 cm^{-1} and 2855 cm^{-1} corresponding to the stretching vibration of C-H, while the sharp band at 1744 cm^{-1} indicated the presence of the carbonyl C=O group. The band at 1461 cm^{-1} is associated with the symmetric bending vibration of methyl or methylene groups commonly found in organic molecules. The band at 1162 cm^{-1} indicated the presence of a C-O bond from esters and alcohols. The biodiesel with a viscosity of 4.8 suggests moderate thickness, suitable for many applications, especially in extreme weather conditions such as tropical Africa (Ewunie, 2021).

Fig. 8: Picture of the Biodiesel produced

Response Surface Methodology

Response Surface Methodology (RSM) with a four-level factorial Box-Bahnken Design (BBD) of Design Expert software version 6.0.11 was employed for optimization of the reaction parameters. The design factors are; Catalyst loading (A), Reaction Time (B), Reaction Temperature (°C) and Methanol to Oil volume ratio (D). After conducting the twenty-nine experiments given by the software and, subsequently, coding in the results obtained, the following statistical analysis was arried out.

ANOVA for Quadratic Model

Table 6: ANOVA for Response Surface Quadratic Model

Source	Sum of Squares	DF	Mean Square	F Value	Prob > F	
Model	3248.913	14	232.0652	2.91281	0.0273	**Significant**
A-CatalystLoad	0.140833	1	0.140833	0.001768	0.9671	
B-Reaction Time	128.7075	1	128.7075	1.615496	0.2244	
C-Temperature	0.300833	1	0.300833	0.003776	0.9519	
D-M/O Ratio	212.5208	1	212.5208	2.667495	0.1247	
A2	847.0557	1	847.0557	10.63198	0.0057	
B2	182.3773	1	182.3773	2.289143	0.1525	
C2	1092.425	1	1092.425	13.71177	0.0024	
D2	405.0779	1	405.0779	5.08441	0.0407	
AB	412.09	1	412.09	5.172424	0.0392	
AC	540.5625	1	540.5625	6.784971	0.0208	
AD	2.25	1	2.25	0.028241	0.8689	
BC	92.16	1	92.16	1.156763	0.3003	
BD	31.9225	1	31.9225	0.400681	0.5369	
CD	77.44	1	77.44	0.972003	0.3409	
Residual	1115.388	14	79.67057			
Lack of Fit	747.8	10	74.78	0.813737	0.6413	**Not significant**
Pure Error	367.588	4	91.897			
Correlation Total	4364.301	28	----	------	--------	

Table 7: Fit Statistic

Std. Dev.	8.925837296	R^2	0.744429199
Mean	76.11724138	Adjusted	0.488858398
C.V.	11.72643298	Predicted	-0.118548841
PRESS	4881.68425	Adeq Precision	5.654199742

ANOVA for RSM Result

The Four-level factorial Box-Bahnken Design (BBD) was applied for the RSM analysis. The design factors are: Catalyst loading; A (0.25-2.00g), Reaction Time; B (30-200m), Reaction Temperature; C (40-90^{o}C), Methanol to oil ratio; D. From the regression surface analysis and the analysis of variance (ANOVA), the second-order polynomial equation in terms of actual factors obtained from the multiple regression analysis of the experimental data is expressed as follows;

$Y=91.68+0.11*A+3.27*B-0.16*C-4.21*D-11.43*A^2-5.30*B^2-12.98*C^2-7.90*D^2-10.15*A*B+11.63*A*C+0.75*A*D+4.80*B*C-2.83*B*D-4.40*C*D.$

Where, Y is the response (yield), and A, B, C and D are the actual factors of the studied variables (Muppaneni, et al., 2013).

Table 3 depicts the actual factors of the reaction parameters and the responses obtained from the experiments. Table 8 is the result of ANOVA fitting of the experimental data to a second-order response surface model. The model F value of 2.91 with a small probability value (Prob> F < 0.0050) indicated a high significance of the regression model. It implies that there is only 0.0050% chance that a model F-value could occur due to noise.

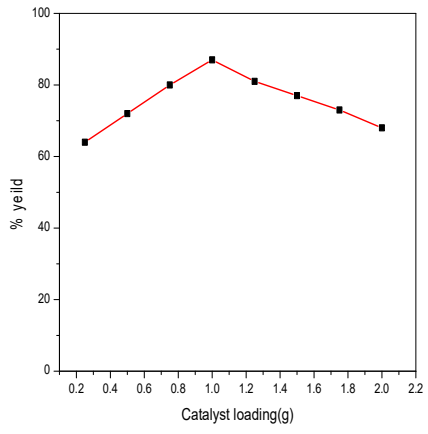

Fig. 9: Effect of catalyst loading

The effect of reaction parameters on biodiesel production

Effect of Catalyst Loading

The effect of catalyst concentration on the percentage yield of biodiesel was determined at different catalyst load (0.25 to 2.00 g) with the same mass of used vegetable oil of 100g, reaction time 90m, methanol to oil molar ratio 3:1 and reaction temperature 60^{o}C. The results of the effect of catalyst concentration on the percentage yield of biodiesel are presented in Figure 9. The results show that there was an increase in the percentage yield of biodiesel up to 87% as the catalyst dosage increased from 0.25 to 1.0g. However, the percentage yield of the biodiesel decreased with a further increase in the catalyst dosage to 68%. This could be attributed to the saturation of the active sites of the catalyst or the possible leaching of the catalyst material back in to the reaction mixture.

3.92 Effect of reaction time

The effect of reaction time on biodiesel yield was evaluated. The reaction times of the experiments were varied (30 to 200 min.) while other parameters; catalyst load of 1.0 g, temperature (60 ^{o}C), and methanol/oil ratio of 6:1 were fixed. The result is represented in Figure 10. An increase in the percentage yield of biodiesel was observed when the reaction time was increased. The maximum yield was achieved at 90 minutes after which further increase in the reaction time did not increase the percentage yield of the biodiesel. This decrease in the yield of biodiesel beyond 90

minutes of reaction time could be associated with reversible reactions resulting in the loss of biodiesel product [Chen et al., 2000 & Mathiyazhagan and Ganapathi 2011).

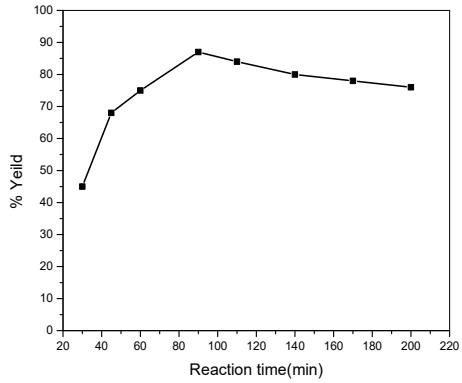

Fig. 10: Effect of reaction time

Effect of oil to methanol ratio

Eight experiments were conducted whereby the methanol/oil ratio was varied (1:3, 1:4, 1:5, 1:6, 1:7, 1:8 and 1:9) to ascertain the effect of methanol/oil ratio on the biodiesel yield. Other reaction parameters; catalyst load (1.0 g), reaction time (90 m), and temperature (60 ºC) were fixed. The results of experiments conducted to determine the effect of the methanol-to-oil ratio are presented in represented on Fig. 11. The result shows that as the methanol-to-oil ratio increases from 1:3 to 1:6, the percentage yield of the biodiesel increases from 49 to 87%. Further increase in methanol to oil ratio decreases the percentage yield to 81% (Ding, et al, 2018, Chuepeng & Komintarachat 2018, Etim 2022).

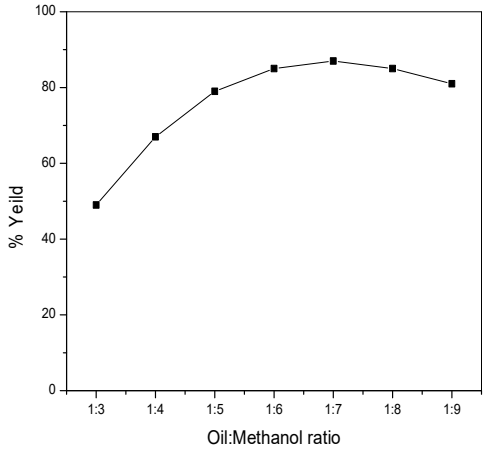

Fig. 11: Effect of oil/methanol ratio

Effect of Reaction Temperature

The reaction temperature is an important parameter that affects the yield of biodiesel. As it can be seen in Fig. 12, by increasing the reaction temperature from 50ºC, the biodiesel yield increased to a maximum of 87 %. Above that temperature, the yield decreased to 78%. This could be attributed to the vaporization of the methanol (Nayak and Vyas, 2022).

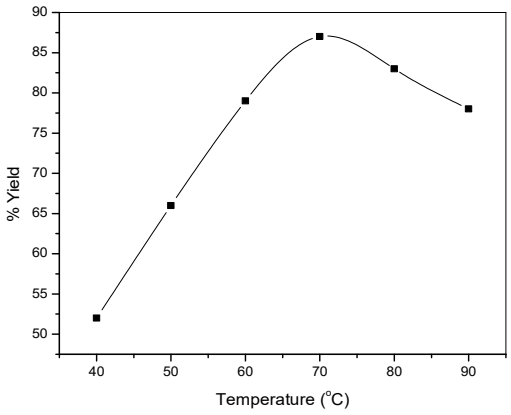

Fig. 12: Effect of reaction temperature

Conclusion

Iron sand was utilized as a precursor to prepare activated Fe_3O_4 catalyst which was characterized and used for the conversion of used cooking oil to biodiesel. The biodiesel produced was successfully isolated and analyzed using various spectroscopic and physicochemical methods. Under Optimized reaction conditions, 87% yield for biodiesel was obtained with a decrease of 10.3% biodiesel yield after the second reuse of the catalyst.

Funding

The research was funded by the Tertiary Education Trust Fund (TetFund) under an Institution Based Research grant (IBR).

Acknowledgments

We sincerely acknowledge the funding of the research by the Tertiary Education Trust Fund (Tetfund) under the Institution Based Research Grant (IBR). The support and contribution of the staff of the Department of Chemistry at Umaru Musa Yaradua University is appreciated.

Conflicts of Interest

The authors declare that there is no conflict of interest in writing this article.

References

Adak, E. S.; Demir, Ö. and Ucar, D. (2020). A Review of the Biodiesel Sources and Production Methods. *International Journal of Energy and Smart Grid (IJESG),* Vol 5(1). ISSN: 2548-0332 e-ISSN 2636-7904.

Andimutiafitri, "Synthesis of Magnetite Based Iron Sand By Using Coprecipitation method." IOSR Journal of Applied Physics (IOSR-JAP)10 (3), 2018, pp. 40-42 www.iosrjournals.org. DOI: 10.9790/4861-1003034042.

Angassa, K., Tesfay, E., Weldmichael, T. G., & Kebede, S. (2023). Research Article Response Surface Methodology Process Optimization of Biodiesel Production from Castor Seed Oil. Hindawi Journal of Chemistry Volume 2023, Article ID 6657732.

Chen J.S., Wang F.Y., Li.X.D.,& Song J.J.,(2000) Geoagraphical variations of trace elements in sediments of the major rivers in eastern china. *Environmental Geology*, 39, 1334-1340. https://doi.org/10.1007/s002540000224

Chuepeng, S., & Komintarachat, C. (2018). Interesterification optimization of waste cooking oil and ethyl acetate over homogeneous catalyst for biofuel production with engine validation. *Applied energy*, *232*, 728-739, https://doi.org/10.1016/j.apenergy.2018.09.085

Ding, H., Ye, W., Wang, Y., Wang, X., Li, L., Liu, D. & Ji, N. (2018). Process intensification of transesterification for biodiesel production from palm oil: Microwave irradiation on transesterification reaction catalyzed by acidic imidazolium ionic liquids. *Energy, 144, 957-967*.

Etim, A. O. (2022). Experimental and computational exploration of advanced biodiesel fuels and hybridisation process evaluation of feedstocks and their chemical combinations (Doctoral dissertation).

Ewunie, G. A., Morken, J., Lekang, O. I., & Yigezu, Z. D. (2021). Factors affecting the potential of Jatropha curcas for sustainable biodiesel production: A critical review. *Renewable and Sustainable Energy Reviews*, *137*, 110500. https://doi.org/10.1016/j.rser.2020.110500

Fahlepy, M. R., Wahyuni, Y., Andhika, M., Vistarani, A. T., & Subaer, S. (2019). Synthesis and Characterization of Nanopraticle Hematite (α-Fe2O3) Minerals from Natural Iron Sand Using Co-Precipitation Method and its Potential Applications as Extrinsic Semiconductor Materials Type-N. In *Materials Science Forum* (Vol. 967, pp. 259-266). Trans Tech Publications Ltd. https://doi.org/10.4028/www.scientific.net/MSF.967.259.

Mahlia, T. M. I., Syazmi, Z. A. H. S., Mofijur, M., Abas, A. E. P., Bilad, M. R., et al. (2020). Patent landscape review on biodiesel production: technology updates. Renew. Sust. Energ. Rev. 118:109526. https://doi.org/10.1016/j.rser

Mathiyazhagan, M., & Ganapathi, A. (2011) Factors Affecting Biodiesel Production *Research in Plant Biology*, 1(2): 01-05.

Muppaneni, T., Reddy, H. K., Ponnusamy, S., Patil, P. D., Sun, Y., Dailey, P., & Deng, S. (2013). Optimization of biodiesel production from palm oil under supercritical ethanol conditions using hexane as co-solvent: A response surface methodology approach. *Fuel*, *107*, 63. https://doi.org/10.1016/j.fuel.2012.11.046.

Nabgan, W., Jalil, A. A., Nabgan, B., Jadhav, A. H., Ikram, M., Ul-Hamid, A., ... & Hassan, N. S. (2022). Sustainable biodiesel generation through catalytic transesterification of waste sources: a literature review and bibliometric survey.

Najmi, M. I., Sunaryono, S., Latifah, E., Taufiq, A., Mufti, N., & Chusna, N. M. (2024). Identification of Crystal Structure, Surface Area, and Magnetic Properties of Nanocomposites. In Journal of Metastable and Nanocrystalline Materials (Vol. 38, pp. 23–30). Trans Tech Publications, Ltd. https://doi.org/10.4028/p-glu976

Nayak, M. G., & Vyas, A. P. (2022). Parametric study and optimization of microwave assisted biodiesel synthesis from Argemone Mexicana oil using response surface methodology. *Chemical Engineering and Processing-Process Intensification*, *170*, 108665. https://doi.org/10.1016/j.cep.2021.108665.

Nugraha P.A., Sari S.P., Hidayati W.N., Dewi C.R., & Kusuma D.Y., (2016) The origin and composition of iron sand deposite in south coast of Yogyarkta. In AIP conference proceedings vol. 1746(1) AIP publishing https://doi.org/10.1063/1.4953953.

Ong, H. C., Masjuki, H. H., Mahlia, T. M. I., Silitonga, A. S., Chong, W. T., and Yusaf, T. (2014). Engine performance and emissions using Jatropha curcas, Ceiba pentandra and Calophyllum inophyllum biodiesel in a CI diesel engine. Energy 69, 427–445. https://doi.org/10.1016/j.energy.2014.03.035.

Prameswari, J., Widayat, W., Buchori, L., & Hadiyanto, H. (2023). Novel iron sand-derived α-Fe_2O_3/CaO_2 bifunctional catalyst for waste cooking oil-based biodiesel production. *Environmental Science and Pollution Research*, *30*(44), 98832-98847. https://doi.org/10.1007/s11356-022-21942-z.

Rahmawati, R; Taufiq, A; Sunaryono, S; Fuad, A; Yuliarto, B; Suyatman, S

and D. Kurniadi, D. “Synthesis of Magnetite (Fe_3O_4) Nanoparticles from Iron sands by Coprecipitation-Ultrasonic Irradiation Methods”, (2018). Journal of Materials and Environmental Sciences. Volume 9, Issue 1, Page 155-160. https://doi.org/10.26872/jmes.2018.9.1.19

Safitri I., Wibowo Y.G., & Rosarina D. (2021). Synthesis and charecterisation of magnetite (Fe_3O_4) nanoparticles from iron sand in Batangari Beach. In IOP conference series: Materials Science and Engineering vol. 1011(1) 012020. IOP publishing. https://doi.org/10.1088/1757-899X/1011/1/012020

Uzun, B. B., Kılıç, M., Özbay, N., Pütün, A. E., & Pütün, E. (2012). Biodiesel production from waste frying oils: Optimization of reaction parameters and determination of fuel properties. *Energy*, *44*(1), 347-35. https://doi.org/10.1016/j.energy.2012.06.024.

Widodo R, Priyono, Rusiyanto, Anis, Ichwani, Setiawan, Fitriyana, Rochman, L, (2020). Synthesis and characterization of iron (III) oxide from natural iron sand of the south coastal area, Purworejo Central Java. Journal of Physics: Conference Series. doi:10.1088/1742-6596/1444/1/012043

Yulianto, A., Bijaksana, S., & Loeksmanto, W. (2003). Comparative study on magnetic characterization of iron sand from several locations in Central Java. *Indonesian Journal of Physics*, *14*(2), 63-66.